Stochastic Analysis of User-Centric Network MIMO

Caiyi Zhu and Wei Yu
The Edward S. Rogers Sr. Department of Electrical and Computer Engineering
University of Toronto, Toronto, ON, M5S 3G4, Canada
Email: caiyi.zhu@mail.utoronto.ca, weiyu@comm.utoronto.ca

***Abstract*—This paper provides an analytical performance characterization of user-centric cooperation for network multiple-input multiple-output (MIMO) systems, where base-stations (BSs) form *finite-sized* clusters to jointly transmit information to and receive information from multiple mobile users. In the user-centric model, the cooperation BS cluster for each user is formed individually and may overlap with each other. The size of clusters determines the amount of backhaul and channel state information needed for implementation. The BSs are equipped with multiple antennas; multiple single-antenna users are served simultaneously; the cooperating BSs perform zero-forcing beamforming across the cluster. By using a stochastic geometry model where the BSs and the users form Poisson point processes over the two-dimensional plane and by further approximating both the signal and interference powers using Gamma distributions of appropriate parameters, this paper shows that, network MIMO provides sum-rate gain for both uplink (UL) and downlink (DL) transmission as compared to single-cell processing. The sum-rate gain is about 30%-60% for a cluster size of 10 and is larger in DL than UL in a typical deployment due to the larger DL transmit power. More significantly, network MIMO can provide 300% gain or more for cluster-edge users, but only for the DL and only with user-centric clustering. This highlights the conclusion that performance evaluation for network MIMO should focus on DL cluster-edge users and on the user-centric clustering strategy.**

I. Introduction

Intercell interference is the main limiting factor in the physical-layer of modern wireless cellular networks with densely deployed base-stations (BSs). Network multiple-input multiple-output (MIMO) is a promising technique for interference mitigation in which BSs jointly transmit information to and receive information from the multiple users via coherent beamforming across multiple BSs [1], [2]. This paper aims to provide analytic modeling and performance characterization of network MIMO systems with finite cluster size.

This paper focuses on the *user-centric* clustering strategies for network MIMO, where a BS cooperation cluster is formed for each user individually, and clusters for different users can partially overlap. Such a clustering strategy allows the user to be always placed at the center of its cluster, so that signal strength is improved and inter-cluster interference reduced.

The main goal of this paper is to quantify the performance of user-centric network MIMO architecture in both uplink (UL) and downlink (DL) as function of cooperation cluster size, which is an indication of the amount of backhaul and channel state information (CSI) needed in implementation. Toward this end, we assume the use of zero-forcing beamforming (ZFBF) strategy across the cluster with equal power allocation across the beams, and adopt a stochastic geometry model of the BS and user locations and a Gamma distribution approximation of the direct and interfering channel strength in order to facilitate an analytic characterization of the average user rate. Perfect and instantaneous CSI is assumed to be available to the BSs within the cluster and also to the users.

A. Related Work

Existing performance evaluation of network MIMO systems has been mostly carried out either using simplified Wyner model or by simulation; and most earlier works have focused on the optimization of transmit strategies for network MIMO systems. For example, [3] numerically studies the throughput performance of network MIMO systems with disjoint clustering, while for user-centric clustering, first proposed in [4], most existing works are based on numerical investigation and optimization strategies that select the best serving cluster of BSs for each user [5], [6], [7].

The performance analysis of network MIMO systems is a challenging task, because cooperating BSs in a network MIMO system typically have different path-loss to the user, so traditional analytic tools for MIMO system, such as the random matrix theory, are not ideally suited to analyze the network MIMO system performance, unless certain symmetry and simplifying assumptions are adopted [8].

To account for the distance dependent path-loss in wireless communication networks, stochastic geometry has recently emerged as a powerful tool for analyzing wireless networks with *random deployment* of BSs and users that are assumed to form Poisson point processes [9], [10]. The application of stochastic geometry to multicell network is however challenging, because of the need to model the effect of beamforming. Toward this end, [11], [12] propose a series of techniques that allow an approximate characterization of the effect of zero-forcing beamforming for multicell networks. This enables a subsequent stochastic analysis of network MIMO systems to be carried out [13]. In particular, instead of a typical coverage probability analysis, [13] provides derivation of a more useful ergodic sum rate expression for a DL network MIMO system with disjoint clustering.

This paper extends the analysis of network MIMO system in [13] to the user-centric clustering case and to both UL and DL. The user-centric case is more complicated, because the beamforming vectors overlap with each other. The analytic performance characterizations of this paper help illustrate the benefit of user-centric clustering as compared to disjoint clustering for both UL and DL scenarios.

B. Main Contributions

The main contributions of this paper are as follows:

1) This paper provides computationally efficient methods for evaluating user rates in both UL and DL network MIMO systems under either disjoint clustering or user-centric clustering under a stochastic model.
2) This paper quantifies the gain of BS cooperation as a function of cooperation cluster size. We see that in term of the average per-cell sum-rate gain, at average cooperation cluster size of 10 (requiring 10 times the backhaul as compared to single-cell processing), the network MIMO system provides about 30% gain for UL under disjoint clustering, 50% gain for UL under user-centric clustering, and 60% gain for DL under either clustering strategies. The gain in DL is larger because of the typical larger DL transmission power at the BSs. User-centric clustering provides benefit, because it places every user at the cluster center, resulting in strong signal power and potentially less interference.
3) The most significant benefit of network MIMO is in term of the cluster-edge performance, but only for the DL and only with user-centric clustering. At average cooperation cluster size of 10, DL network MIMO with user-centric clustering improves 10th-percentile user rate of the system by factor of three, even when compared to disjoint clustering. This is due to the significant capability of user-centric strategy for reducing inter-cluster interference.

II. System Model

Consider a wireless cellular network in which each BS is equipped with M antennas and each user is equipped with a single antenna. A user is associated with the BS with the strongest average channel. We assume that user density is much larger than BS density, so that each BS is associated with many users. Among all its associated users, each BS schedules $K < M$ users in each time slot. We assume round-robin scheduling for simplicity. We assume flat-fading channels with full frequency reuse, i.e., transmissions from neighboring cells cause mutual interference to each other.

This paper aims to analyze the performance of network MIMO systems in which each user is jointly served by a cooperative cluster of BSs. In the *disjoint clustering* scheme, the set of BSs are partitioned into disjoint clusters; each user is served by the cluster of BSs to which its associated BS belongs. In *user-centric clustering*, each scheduled user forms an individually chosen cluster of serving BSs based on average channel strength; the clusters for different users can partially overlap. Fig. 1 illustrates disjoint vs. user-centric clustering.

Let Θ_i denote the cooperative cluster of serving BSs for user i. Let B_i be the cluster size, i.e., $B_i = |\Theta_i|$. Recall that each BS in Θ_i schedules K of its associated users. We denote the set of all users scheduled by the BSs in user i's serving cluster as Ω_i, so that $|\Omega_i| = KB_i$. In the rest of the paper, user i is called the typical user. The other $KB_i - 1$ users in Ω_i are called intra-cluster users of user i. All the rest of the users in the network are termed inter-cluster users.

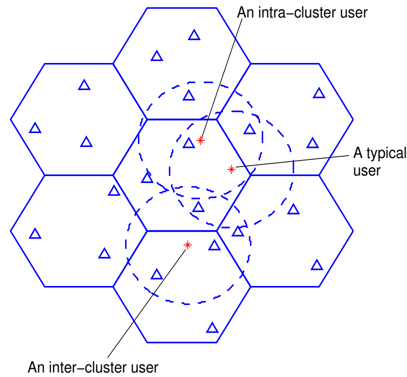

Fig. 1. Disjoint vs. user-centric clustering: The BSs are denoted by triangles, the users by stars. Under disjoint clustering, the serving BSs form non-overlapping cooperative clusters, shown in this example by the hexagonal region. Under user-centric clustering, the serving BSs are formed for each user individually, shown in this example by the dotted circles.

This paper assumes the use of ZFBF in both UL and DL, in which a beamformer for the typical user i is designed across its serving BSs in Θ_i to null interference from/to all intra-cluster users. Below we describe the ZFBF design in UL in detail. The DL model is similar.

In uplink ZFBF, the message from the typical user i is jointly decoded across the BSs in Θ_i, while interference from all intra-cluster users in Ω_i is nulled. Let $\boldsymbol{y}_i \in \mathbb{C}^{MB_i}$ be the received signal across all the serving BSs of user i:

$$\begin{aligned}\boldsymbol{y}_i &= \sum_j \boldsymbol{h}_{ij} x_j + \boldsymbol{z} \qquad (1)\\ &= \underbrace{\boldsymbol{h}_{ii} x_i}_{signal} + \underbrace{\sum_{m \neq i, m \in \Omega_i} \boldsymbol{h}_{im} x_m}_{\text{intra-cluster interference}} + \underbrace{\sum_{j \notin \Omega_i} \boldsymbol{h}_{ij} x_j}_{\text{inter-cluster interference}} + \boldsymbol{z}\end{aligned}$$

where $\boldsymbol{h}_{ij}^H = [\cdots \boldsymbol{g}_{bj}^H \cdots]_{b \in \Theta_i}$ denotes the collective vector channel between user j and the set of serving BSs of user i, and $\boldsymbol{g}_{bj} \in \mathbb{C}^M$ denotes the channel between user j and BS b. Here, x_j is the transmit signal of user j with power normalized to 1, i.e., $\mathbb{E}[x_j^2] = 1$. Finally, $\boldsymbol{z} \sim \mathcal{CN}(0, \sigma_u^2 \boldsymbol{I}_{MB_i})$ is the background noise at the BSs including thermal noise and other possible sources of interference and scaled to account for transmit power normalization.

The ZF receive beamformer for user i is designed to be orthogonal to the transmission from the $KB_i - 1$ intra-cluster users, so that the interference from these users is completely eliminated. In particular, the normalized ZF receive beamformer for user i is chosen to be the following:

$$\boldsymbol{w}_i = \frac{(\boldsymbol{I}_{MB_i} - \boldsymbol{H}_{-i}\boldsymbol{H}_{-i}^\dagger)\boldsymbol{h}_{ii}}{\|(\boldsymbol{I}_{MB_i} - \boldsymbol{H}_{-i}\boldsymbol{H}_{-i}^\dagger)\boldsymbol{h}_{ii}\|_2}, \qquad (2)$$

where $\boldsymbol{H}_{-i} = [\cdots \boldsymbol{h}_{ij} \cdots]_{j \neq i, j \in \Omega_i}$ denotes the channel matrix between the serving BSs of user i and its $KB_i - 1$ intra-cluster users. It is easy to see that the column space of the matrix

$(\boldsymbol{I}_{MB_i} - \boldsymbol{H}_{-i}\boldsymbol{H}_{-i}^{\dagger})$ is the null space of $\boldsymbol{H}_{-i}$. By projecting the direct channel $\boldsymbol{h}_{ii}$ onto the null space of $\boldsymbol{H}_{-i}$, the signal power is maximized while the required orthogonality is guaranteed.

The signal-to-interference-and-noise ratio (SINR) of user i can now be stated as follows:

$$\gamma_i = \frac{|\boldsymbol{w}_i^H \boldsymbol{h}_{ii}|^2}{\sum_{j \notin \Omega_i} |\boldsymbol{w}_i^H \boldsymbol{h}_{ij}|^2 + \sigma_u^2}. \tag{3}$$

Observe that in user-centric clustering, each user is always at the center of its serving BSs. Since the channel strength is a function of the distance, the signal power in the user-centric case is equivalent to that of a cluster-center user in disjoint clustering, and much larger than that of a cluster-edge user. Thus on average, user-centric clustering has an advantage in term of signal power as compared to disjoint clustering. This holds for both UL and DL.

However in term of interference power, user-centric clustering brings much more benefit in DL than UL. This is because in UL, the interference seen at the serving BSs is about the same regardless of the clustering strategy, while in the DL, the cluster-edge users tend to see significantly less interference due to user-centric clustering.

III. Stochastic Geometry Analysis

In order to provide an analytic performance characterization of network MIMO systems, this paper proposes a statistical model of cellular networks accounting for both the random geographic locations of the BSs and the users, as well as the channel fading.

The channel from BS b to user i is modeled as $\boldsymbol{g}_{bi} = \sqrt{\beta_{bi}}\boldsymbol{f}_{bi} \in \mathbb{C}^{M\times 1}$. The distance-dependent pathloss component is modeled as $\beta_{bi} = (1 + r_{bi}/d_0)^{-\alpha}$, where r_{bi} is the distance between the BS b and user i, d_0 is a reference distance, and α is the pathloss exponent. The Rayleigh fading component is modeled as $\boldsymbol{f}_{bi} \sim \mathcal{CN}(0, \boldsymbol{I}_M)$.

We use stochastic geometry to account for the pathloss and use a Gamma distribution approximation to analyze the overall performance. In particular, the BSs are randomly placed over a two-dimensional plane as a homogenous Poisson Point Process (PPP) with a fixed intensity λ_b, denoted as Φ_b. The users are also randomly placed as a PPP. The users are associated with the strongest BS; each BS schedules K active users from the set of associated users. Technically the active users no longer form a PPP. But to enable the averaging over user locations, we further approximate that the active users form a PPP, Φ_u, with intensity $\lambda_u = K\lambda_b$.

We model user-centric clustering as follows: each user chooses its BS cooperation cluster based on distance. In particular, the user i's BS cooperation cluster is $\Theta_i = \Phi_b \cap \mathcal{B}_{x_u}(R)$, where $\mathcal{B}_{x_u}(R)$ denotes a circle of radius R centered at user i whose location is denoted as x_u.

We now carry out a stochastic analysis of uplink user-centric network MIMO system. Note that we do not perform power control. In the uplink, all users transmit at a fixed power. (Similarly in the downlink analysis, each downlink beam transmits at a fixed power.)

1) Signal Strength in UL: The channel strength of the intended signal for the typical user is:

$$\begin{aligned} \|\boldsymbol{h}_{11}\|^2 &= \sum_{b\in\Theta_1} \boldsymbol{g}_{b1}^H \boldsymbol{g}_{b1} \\ &= \sum_{b\in\Theta_1} \beta_{b1} \boldsymbol{f}_{b1}^H \boldsymbol{f}_{b1} \sim \sum_{b\in\Theta_1} \Gamma\left(M, \beta_{b1}\right). \end{aligned} \tag{4}$$

Since the entries of the MIMO channels are Gaussian distributed, the overall magnitude of the channel between the typical user and its set of cooperating BSs is a sum of Gamma random variables with different scale parameters depending on the distances between the user and the BSs. We proceed to approximate the above distribution into a form amendable to stochastic geometry analysis. The series of approximations below are developed in part in [11], [12], [13].

The analysis first uses a technique pioneered in [11] for approximating the sum of Gamma distributions as a single Gamma distribution with shape and scale parameters determined by matching the first and second order moments. For the channel $\|\boldsymbol{h}_{11}\|^2$ in (4), this approximation leads to $\|\boldsymbol{h}_{11}\|^2 \sim \Gamma(k_1, \theta_1)$ with

$$k_1 = M\frac{\left(\sum_{b\in\Theta_1}\beta_{b1}\right)^2}{\sum_{b\in\Theta_1}\beta_{b1}^2}, \quad \theta_1 = \frac{\sum_{b\in\Theta_1}\beta_{b1}^2}{\sum_{b\in\Theta_1}\beta_{b1}}. \tag{5}$$

To obtain signal power, we need to further project the channel vector onto the beamforming vector. The exact signal power distribution resulting from such a projection is not easy to characterize. Instead, we adopt a second approximation by drawing a parallel with the following fact on the projection of an isotropic channel vector to a lower dimensional space (although our actual channel is not isotropic).

If a channel vector $\boldsymbol{h} \in \mathbb{C}^N$ were isotropic in the N-dimensional space such that $\|\boldsymbol{h}\|^2 \sim \Gamma(N, \theta)$, then the projection of $\boldsymbol{h}$ onto a P-dimensional subspace results in a Gamma distribution $\Gamma(P, \theta)$. In other words, the shape parameter is scaled by P/N, while the scale parameter is kept the same.

Now, to obtain an approximate signal power distribution after the projection to ZF beamformer, we apply the same scaling of the shape parameter even when the channel is non-isotropic. This same approximation technique is also used in [12], [13]. Specifically in our case, $\|\boldsymbol{h}_{11}\|^2 \sim \Gamma(k_1, \theta_1)$. To project the channel vector onto the ZF beamforming vector, we note that the receive beam of the user lies in the null space of the subspace spanned by the $KB_1 - 1$ interfering channel vectors. Therefore, the shape parameter for the signal power after projection must be scaled by $\frac{MB_1 - KB_1 + 1}{MB_1}$. The signal power distribution can therefore be approximated as:

$$\zeta_1^{(UL)} = |\boldsymbol{w}_1^H \boldsymbol{h}_{11}|^2 \sim \Gamma\left(\frac{MB_1 - KB_1 + 1}{MB_1}k_1, \theta_1\right). \tag{6}$$

Recall that the number of BSs in the cluster B_1 is a Poisson random variable with mean $\bar{B} = \lambda_b^2 \pi R^2$. To make the analysis tractable, we replace B_1 by its mean $\bar{B}$ as a further approximation.

Finally, the distribution above has parameters that depend on the BS location. To facilitate a stochastic geometry analysis, we decompose the above signal distribution as a linear combination of independent Gamma distributions. Using again the technique of matching the first and second moments, the signal power can now be approximated as follows [13]:

$$\zeta_1^{(UL)} = |\boldsymbol{w}_1^H \boldsymbol{h}_{11}|^2 \approx \sum_{b\in\Theta_1} \beta_{b1} G_{b1}^{(\varpi)} \tag{7}$$

where $G_{bj}^{(\varpi)}$ are i.i.d. random variables distributed as $\Gamma(\varpi, 1)$, where $\varpi = \frac{M\bar{B}-K\bar{B}+1}{M\bar{B}}$. Here, we also use the fact that if $X \sim \Gamma(k, \theta)$, then $cX \sim \Gamma(k, c\theta)$ for any positive c.

2) Interference Strength in UL: As intra-cluster interference is eliminated with ZF receiver, the residual interference only comes from inter-cluster users. In deriving the distribution of aggregate interference, we first investigate the interference from a single user j, then sum up the interference over all inter-cluster users.

Similar to the analysis of (5), the interfering channel strength can also be approximated as a Gamma random variable using the moment matching technique as follows:

$$\|\boldsymbol{h}_{1j}\|^2 = \sum_{b\in\Theta_1} \boldsymbol{g}_{bj}^H \boldsymbol{g}_{bj} \sim \sum_{b\in\Theta_1} \Gamma(M, \beta_{bj}) \approx \Gamma(k_{1j}, \theta_{1j}), \tag{8}$$

where

$$k_{1j} = M \frac{\left(\sum_{b\in\Theta_1} \beta_{bj}\right)^2}{\sum_{b\in\Theta_1} \beta_{bj}^2}, \theta_{1j} = \frac{\sum_{b\in\Theta_1} \beta_{bj}^2}{\sum_{b\in\Theta_1} \beta_{bj}}. \tag{9}$$

To project the interference signal onto the receive beamformer $\boldsymbol{w}_1$, (which is a one-dimensional subspace independent of the interfering channel vector $\boldsymbol{h}_{1j}$ of dimension MB_1), we again approximate the channel vector as isotropic. The projection then results in the scaling of the shape parameter of the interference as $\frac{k_{1j}}{MB_1}$. Finally, we replace B_1 by its mean $\bar{B}$, then decompose the interference into linear combination of independent Gamma distributions again using the moment matching technique as:

$$\nu_{1j}^{(UL)} = |\boldsymbol{w}_1^H \boldsymbol{h}_{1j}|^2 \approx \sum_{b\in\Theta_1} \beta_{bj} G_{bj}^{(\frac{1}{\bar{B}})}, \tag{10}$$

where $G_{bj}^{(\frac{1}{\bar{B}})}$ are i.i.d. $\Gamma\left(\frac{1}{\bar{B}}, 1\right)$ distributed.

The aggregate residual interference is the sum of interference from all inter-cluster users. We approximate these users as outside of $\mathcal{B}_o(R)$. The aggregate interference is now

$$\nu_1^{(UL)} = \sum_{j\notin\Omega_1} \nu_{1j} \approx \sum_{j\notin\Omega_1} \sum_{b\in\Theta_1} \beta_{bj} G_{bj}^{(\frac{1}{\bar{B}})}. \tag{11}$$

3) Ergodic Rate in UL: The ergodic rate of the typical user in the UL user-centric network MIMO system can now be derived using tools from stochastic geometry by using the signal and interference power distributions (7) and (11) with $\Theta_1 = \Phi_b \cap \mathcal{B}_o(R)$ and $\Omega_1 = \Phi_u \cap \mathcal{B}_o(R)$. The achievable rate of the user is computed as $\log(1 + \mathrm{SINR})$. By utilizing the following expression of the log function in term of integral [14, Lemma 1]

$$\ln(1 + x) = \int_0^\infty \frac{e^{-z}}{z}(1 - e^{-xz})\mathrm{d}z, \tag{12}$$

the ergodic rate averaged over the distributions of Φ_b and Φ_u, can be obtained as follows [14]:

$$\bar{C}_U = \int_0^\infty \frac{e^{-s\sigma^2}}{s} L_{\nu_1^{(UL)}}(s) \left(1 - L_{\zeta_1^{(UL)}}(s)\right) \mathrm{d}s, \tag{13}$$

where $L_{\zeta_1^{(UL)}}(s)$, $L_{\nu_1^{(UL)}}(s)$ are respectively the Laplace transforms of signal and interference power distributions, which can be explicitly computed using stochastic geometry.

The above analysis is for the UL. A similar DL analysis can also be carried out, and likewise for disjoint clustering for both UL and DL as well. We refer the readers to the full version of the paper [15] for details.

IV. User-Centric vs. Disjoint Clustering

This section provides numerical results for a stochastic deployment of BSs in a cellular network, where each BS is equipped with 4 antennas and schedules 2 single-antenna users, i.e., $M = 4, K = 2$. The power of the transmit beam for each user in the DL is set to be 40 dBm over 20MHz bandwidth. The transmit power of each user in UL is 23dBm over 20MHz. Power spectrum density of the background noise is set to -174dBm/Hz; a noise figure of 9dB and an SINR gap of 3dB are included. We use a pathloss model of $128.1 + 37.6\log(d)$ in dB, where d is expressed in km.

Figs. 2 and 3 show the UL and DL ergodic user rate evaluated from the analytical expressions as well as obtained from system-level simulation for both user-centric and disjoint clustering cases. For numerical comparison, we include both the simulation results with Poisson number of BSs as well as the case with fixed number of exactly $\bar{B}$ BSs in the cluster.

We observe that the analytical results match with the simulation within an accuracy of about 5%, which is remarkable given the number of approximations involved in the analysis. As expected, the ergodic rate increases as the cluster size grows, but larger cluster benefits in DL more than UL. This is because DL transmit power is larger, so it is more interference limited than UL. Consequently, interference mitigation brings more improvement to the DL.

Moreover, user-centric clustering achieves higher ergodic rate than disjoint clustering for both UL and DL. The benefit of user-centric cluster in UL is about 15-20%, and in DL only about 5%. User-centric clustering enhances signal power for both UL and DL. But in term of interference, user-centric clustering may actually increase interference for some cluster-center users in the DL, while reducing interference for DL cluster-edge users.

We should note that at average cooperation cluster size of 10, i.e., at the cost of sharing 10 times as much data in the backhaul, the network MIMO system provides only modest gain: about 30% for UL under disjoint clustering, 50% for

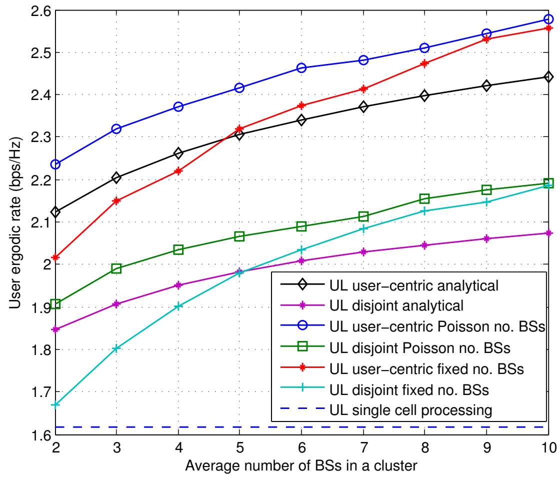

Fig. 2. Ergodic user rate for UL network MIMO systems.

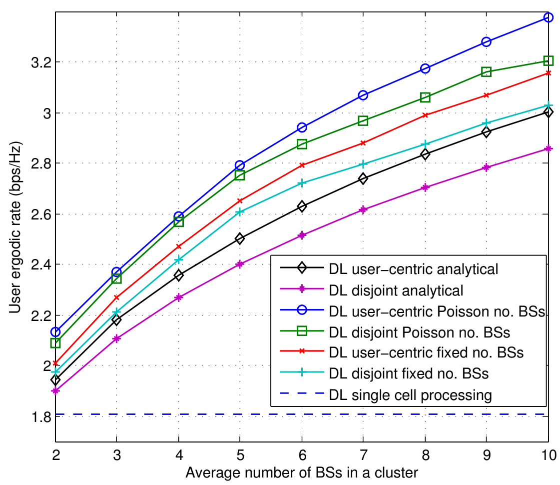

Fig. 3. Ergodic user rate for DL network MIMO systems.

UL under user-centric clustering, and 60% gain for DL under either clustering strategies.

For cluster-edge users, the benefit of network MIMO is much more significant. As shown in the cumulative distribution function (CDF) plot in Fig. 4, the 10th-percentile user rate performance for DL user-centric clustering can improve as compared to disjoint clustering by a factor of three at $\bar{B} = 10$. This provides strong justification for DL user-centric network MIMO. We note that such benefit does not occur in UL.

V. Conclusion

This paper analyzes the system performance of user-centric network MIMO system with zero-forcing beamforming across multiple BSs. By using stochastic geometry and by approximating the channel and interference power distributions, we derive tractable analytical expressions of ergodic rates. The main insight of this paper is that considering the significant cost of backhaul provisioning, the design of future cooperative wireless cellular communication networks should focus on cluster-edge users and with user-centric clustering in the DL.

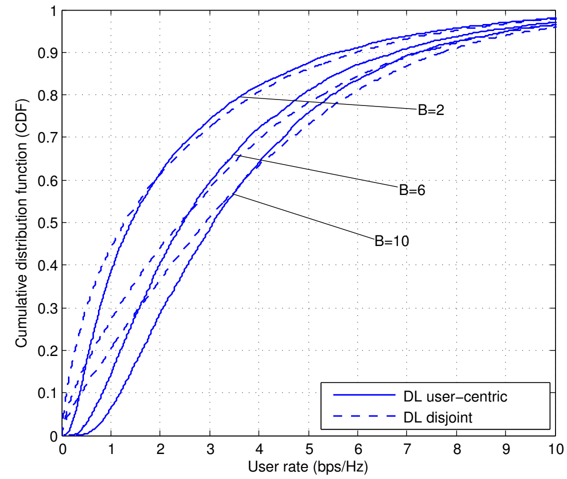

Fig. 4. User rate distributions for DL network MIMO systems.

References

[1] M. K. Karakayali, G. J. Foschini, and R. Valenzuela, "Network coordination for spectrally efficient communications in cellular systems," *IEEE Wireless Commun.*, vol. 13, no. 4, pp. 56–61, Aug. 2006.

[2] D. Gesbert, S. Hanly, H. Huang, S. S. Shitz, O. Simeone, and W. Yu, "Multi-cell MIMO cooperative networks: A new look at interference," *IEEE J. Sel. Areas Commun.*, vol. 28, no. 9, pp. 1380–1408, Nov. 2010.

[3] H. Huang, M. Trivellato, A. Hottinen, M. Shafi, P. J. Smith, and R. Valenzuela, "Increasing downlink cellular throughput with limited network MIMO coordination," *IEEE Trans. Wireless Commun.*, vol. 8, no. 6, pp. 2983–2989, 2009.

[4] A. Papadogiannis, D. Gesbert, and E. Hardouin, "A dynamic clustering approach in wireless networks with multi-cell cooperative processing," in *IEEE Inter. Conf. Commun. (ICC)*, 2008, pp. 4033–4037.

[5] C. T. Ng and H. Huang, "Linear precoding in cooperative MIMO cellular networks with limited coordination clusters," *IEEE J. Sel. Areas Commun.*, vol. 28, no. 9, pp. 1446–1454, Dec. 2010.

[6] B. Dai and W. Yu, "Sparse beamforming and user-centric clustering for downlink cloud radio access network," *IEEE Access*, vol. 2, pp. 1326–1339, Nov. 2014.

[7] D. Su and C. Yang, "User-centric downlink cooperative transmission with orthogonal beamforming based limited feedback," *IEEE Trans. Commun.*, vol. 63, no. 8, pp. 2996–3007, Aug. 2015.

[8] H. Huh, A. M. Tulino, and G. Caire, "Network MIMO with linear zero-forcing beamforming: Large system analysis, impact of channel estimation, and reduced-complexity scheduling," *IEEE Trans. Inf. Theory*, vol. 58, no. 5, pp. 2911–2934, 2012.

[9] J. G. Andrews, F. Baccelli, and R. K. Ganti, "A tractable approach to coverage and rate in cellular networks," *IEEE Trans. Commun.*, vol. 59, no. 11, pp. 3122–3134, Nov. 2011.

[10] T. D. Novlan, H. S. Dhillon, and J. G. Andrews, "Analytical modeling of uplink cellular networks," *IEEE Trans. Wireless Commun.*, vol. 12, no. 6, pp. 2669–2679, June 2013.

[11] R. W. Heath Jr, T. Wu, Y. H. Kwon, and A. C. Soong, "Multiuser MIMO in distributed antenna systems with out-of-cell interference," *IEEE Trans. Signal Process.*, vol. 59, no. 10, pp. 4885–4899, Oct. 2011.

[12] N. Seifi, R. Heath, M. Coldrey, and T. Svensson, "Adaptive multicell 3D beamforming in multi-antenna cellular networks," *IEEE Trans. Veh. Technol.*, 2016.

[13] K. Hosseini, W. Yu, and R. S. Adve, "A stochastic analysis of network MIMO systems," *IEEE Trans. Signal Process.*, 2016.

[14] Y. Lin and W. Yu, "Downlink spectral efficiency of distributed antenna systems under a stochastic model," *IEEE Trans. Wireless Commun.*, vol. 13, no. 12, pp. 6891–6902, Dec. 2014.

[15] C. Zhu and W. Yu, "Stochastic modeling and analysis of user-centric cooperation in network MIMO systems," manuscript in preparation.